

Electric-Field-Induced Raman Scattering in SrTiO_3 and KTaO_3

P. A. FLEURY AND J. M. WORLOCK

Bell Telephone Laboratories, Holmdel, New Jersey 07733

(Received 1 May 1968)

In their paraelectric phases, SrTiO_3 and KTaO_3 crystallize in the cubic perovskite structure (space group O_h^h) in which the first-order Raman effect is forbidden. We discuss here experiments in which first-order Raman scattering has been induced by the application of an external electric field that serves to remove the center of inversion symmetry of the crystals. An electric field applied along a (001) direction induces a C_4 symmetry in the crystal and renders all the phonons first-order Raman-active. We have studied induced scattering from all four TO phonons in SrTiO_3 and from three TO phonons in KTaO_3 at temperatures between 8 and 300°K and with electric fields between 0.2 to 15 kV/cm. Most attention was given to the lowest-frequency TO phonon—the “soft” or “ferroelectric” mode—whose striking decrease in frequency as the temperature is lowered signals the lattice instability associated with the ferroelectric phase transition. Detailed investigations were also made of the electric field dependence of the soft-mode frequencies in both materials. At 8°K this frequency in SrTiO_3 increases from 10 cm^{-1} at zero field to 45 cm^{-1} at 12 kV/cm. Similar behavior is observed in KTaO_3 . From this behavior we infer values for the nonlinear dielectric response coefficients of the crystals. Some discussion is given of the large discrepancies between the soft-mode linewidths that we observe and those previously obtained from infrared (IR) reflectivity experiments. At 80°K in SrTiO_3 the Raman and IR measurements yield values of 3 and 61.7 cm^{-1} , respectively. Additional topics considered include relative electric-field-induced scattering cross sections for the various phonon modes, and the temperature dependence of the soft-mode linewidth. Finally, the question of anomalous first-order Raman scattering in the intrinsic spectrum of SrTiO_3 , recently reported by several authors, is considered in the light of the field-induced first-order Raman scattering.

I. INTRODUCTION

IN general, only phonons possessing some even-parity character are Raman-active. Yet some very interesting materials are of sufficiently high symmetry that all their long-wavelength phonons are of odd parity—and hence forbidden to exhibit a first-order Raman effect. Included in this class, for example, is the simplest structure known to undergo a ferroelectric phase transition—the cubic perovskite structure exhibited by BaTiO_3 , SrTiO_3 , KTaO_3 , etc., in their paraelectric phases.¹ In recent theories of ferroelectricity,² lattice dynamics (phonon behavior) is of central importance. Hence the powerful technique of Raman scattering in such systems could be quite useful if the selection rules forbidding first-order Raman effect could be relaxed. In this paper, we describe some recent experiments on paraelectric SrTiO_3 and KTaO_3 in which the Raman-forbidden phonons have been made Raman-active by applying an external electric field. Our experimental techniques permit virtually complete discrimination against the intrinsic second-order Raman spectra which in these materials are quite complicated and intense. Thus we have been able to study the first-order Raman spectra at a variety of temperatures (8–300°K) and applied fields (0.2–15 kV/cm). Particular attention has been paid to the lowest-frequency TO phonon—the so-called “ferroelectric mode”—responsible for the ferroelectric phase transition.

In Sec. II, we present the theory necessary to interpret our experiments, including a discussion of the symmetry properties of the perovskites with and without applied fields, as well as an outline of the Devonshire and Cochran models of ferroelectricity.^{2,3}

Section III describes the experimental techniques and apparatus, with particular emphasis on the methods of imposing electric fields and synchronous detection of the scattered intensity.

Our experimental results are presented and discussed in Sec. IV. Observations concerning the ferroelectric (soft) modes in SrTiO_3 and KTaO_3 are presented first. These include the temperature and electric field dependence of the phonon frequency, linewidth, and field-induced scattering cross section. The striking electric field dependence at low temperatures of the soft-mode frequency ω_s is related to the nonlinear effects in the dielectric response of the crystals. Some discussion is presented of the large discrepancies between our measured linewidths and those reported in infrared (IR) results.^{4,5} We have also observed electric-field-induced scattering from other TO phonons as well as the so-called silent mode, which is neither Raman- nor IR-active in absence of external fields. The phonon frequencies that we observe are in excellent agreement with neutron scattering results,^{6,7} although published results do not cover so

³ A. F. Devonshire, *Advan. Phys.* **3**, 85 (1954).

⁴ A. S. Barker, *Phys. Rev.* **145**, 391 (1966).

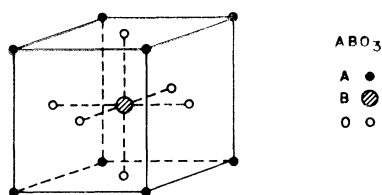
⁵ R. C. Miller and W. G. Spitzer, *Phys. Rev.* **129**, 94 (1963).

⁶ R. A. Cowley, *Phys. Rev.* **134**, A981 (1964).

⁷ G. Shirane, R. Nathans, and V. J. Minkiewicz, *Phys. Rev.* **157**, 396 (1967).

¹ P. Vonsden, *Acta Cryst.* **4**, 373 (1951).

² W. Cochran, *Advan. Phys.* **9**, 387 (1960).

FIG. 1. Cubic perovskite unit cell: ABO_3

wide a temperature range, nor do they present linewidths. We also list the electric-field-induced scattering cross sections at various temperatures for the phonon modes that we observed. Finally, we apply our results to the question of anomalous first-order scattering in the intrinsic spectrum of $SrTiO_3$ —a possibility expressed by several recent investigators. Our conclusion is that the crystal undergoes a phase transition in which the unit cell is doubled in size. Section V concludes the paper with a discussion of the usefulness of electric-field-induced Raman scattering in general and of the application to ferroelectric materials in particular.

II. THEORY

A. Symmetry and Selection Rules

Both $SrTiO_3$ and $KTaO_3$ crystallize in the cubic perovskite structure shown in Fig. 1 (space group O_h^1 or $Pm3m$).¹ The long-wavelength or zero-wave-vector phonons in this crystal are all of odd parity, because each ion occupies a site with inversion symmetry. As a result, first-order Raman scattering is forbidden in the electric-dipole approximation. An external electric field applied in the $[001]$ direction distorts the unit cell, so as to remove all centers of symmetry. The factor group (or point group) then becomes the tetragonal group C_{4v} , and all phonons become Raman-active. Figure 2 shows the symmetry analysis of zero-wave-vector phonons in the cubic perovskites with and without a $[001]$ external field. Of the 15 normal modes in the cubic structure, three are acoustic and three are silent, i.e., neither IR-active nor Raman-active, transforming with the triply degenerate representation F_{2u} (Γ_{25}). In the silent mode, only oxygen atoms move. The remaining nine modes are three sets of triply degenerate IR-active, F_{1u} (Γ_{15}) modes. In fact, long-range Coulomb fields split this triple degeneracy for finite wave vector, so that there are three longitudinal (LO) and three pairs of transverse (TO) optical modes. This splitting is ascribed to the "internal field" in Fig. 2. Because of the TO-LO splitting, it is necessary to be explicit about the phonon wave vector. In our experiments, as shown in the figure, the phonon propagates in the $[\bar{1}10]$ direction.

In the presence of the $[001]$ field the silent mode splits into a nondegenerate B_1 mode, with oxygen motion parallel to the field, and a doubly degenerate

E mode, with oxygen motion perpendicular to the field. The nonzero Raman-tensor components are given in the final column of the figure.

The IR modes each split into one A_1 , with motion parallel to the field (a transverse mode), and one E mode. The degeneracy of the E mode is already broken by the TO-LO splitting mentioned above. Again, the Raman-tensor components for the various modes are shown in the last column of Fig. 2.

The only modes displaying α_{zz} components of the Raman tensor will be the IR-active TO modes polarized parallel to the field, so that these can be unambiguously identified. As will be shown later, the external-field splitting of the TO modes becomes appreciable for the lowest-frequency phonons, so that it is important to separate the TO parallel (α_{zz}) and TO perpendicular (α_{xz}, α_{yz}) components. It is not possible to distinguish between TO and LO IR-active modes in the geometries employed in our experiments. The B_1 silent mode could be observed if the crystal were rotated 45° about the z axis or electric-field direction.

Fortunately, approximate frequencies for all the zone-center phonons in $KTaO_3$ and $SrTiO_3$ are known from IR-reflectivity^{4,5} and cold neutron scattering experiments,^{6,7} so that it is possible, in most cases, to identify the nature of the mode simply by knowing its frequency. We shall, however, make good use of the knowledge of the Raman-tensor components for the field-split TO phonons.

B. Field-Induced Scattering and Shifts of Phonon Frequencies

In the limit of low fields, we should expect that all effects, e.g., cross sections, frequency shifts, should

MODE TYPE	POLARIZATION	REPRESENTATION	SPLITTING	RAMAN TENSOR
IR TO	001	O_h	A_1	$\alpha_{xx}, \alpha_{yy}, \alpha_{zz}$
		C_{4v}	EXTERNAL FIELD	
IR TO	110	F_{1u}	E	α_{xz}, α_{yz}
LO	$\bar{1}10$		INTERNAL FIELD	
SILENT	001	F_{2u}	B_1	$\alpha_{xx} = -\alpha_{yy}$
SILENT	110		EXTERNAL FIELD	
SILENT	$\bar{1}10$		E	α_{xz}, α_{yz}

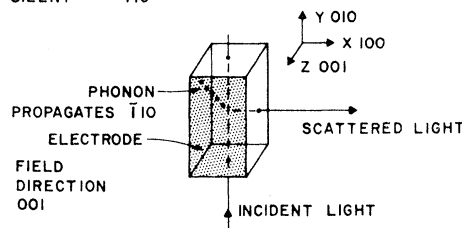


FIG. 2. Tabulation of phonon symmetries in the perovskite structure without external electric field (O_h) and with external field applied along the z direction (C_{4v}). Experimental sample geometry is indicated in the lower part of the figure. See Sec. II A for further discussion.

be quadratic in applied field. Because of the centrosymmetry, no property can change linearly with field. In strong fields, however, these crystals exhibit nonlinear behavior, so that it is necessary to discuss their nonlinear response. Here we shall make use of the Devonshire phenomenological model³ to discuss the low-frequency dielectric behavior of the crystals, and the Lyddane-Sachs-Teller (LST) relation⁸ to connect dielectric response with the phonon frequencies.

In the Devonshire model, the Gibbs free-energy density is expanded in a power series in the lattice polarization:

$$G = G_0(T) + \frac{1}{2}[\chi(T)](P_x^2 + P_y^2 + P_z^2) + \frac{1}{4}\xi(P_x^4 + P_y^4 + P_z^4) + \frac{1}{2}\xi'(P_x^2 P_y^2 + P_y^2 P_z^2 + P_z^2 P_x^2) + \frac{1}{6}\zeta(P_x^6 + P_y^6 + P_z^6) + \text{other sixth-order terms} + \dots \quad (1)$$

The symmetry of the lattice allows only terms which are even in each of the polarization components individually, so that this is the most general expression up to fourth order in polarization. The sixth-order terms not shown are of the form $P_x^2 P_y^2 P_z^2$ and $P_x^2 P_y^4$. The temperature dependence is left quite arbitrary, and is contained in $G_0(T)$, $\chi(T)$, and perhaps, ξ , ξ' , and ζ .

The differential of the Gibbs free-energy function is given by

$$dG = \mathbf{E} \cdot d\mathbf{P} - SdT,$$

so that

$$E_z = (\partial G / \partial P_z)_T \quad \text{and} \quad S = -(\partial G / \partial T)_P.$$

We follow conventional practice and take E to be the macroscopic field inside the sample, which is, except for fringe fields, just the voltage applied to electrodes divided by their separation. Then

$$E_z = \chi(T)P_z + \xi P_z^3 + \xi' P_z(P_x^2 + P_y^2) + \zeta P_z^5 + \dots \quad (2)$$

We can define an incremental inverse dielectric constant, or dielectric tensor, which is appropriate for describing the small signal response of the crystal in the presence of a biasing field:

$$[1/\epsilon_0(\kappa-1)]_{zz} \equiv \partial E_z / \partial P_z = \chi(T) + 3\xi P_z^2 + \xi'(P_x^2 + P_y^2) + 5\zeta P_z^4, \quad (3)$$

$$[1/\epsilon_0(\kappa-1)]_{zx} \equiv \partial E_z / \partial P_x = \partial E_x / \partial P_z = 2\xi' P_x P_z + \dots \quad (4)$$

When the field is applied and polarization is induced in the crystal, the temperature tends to increase; so it is important to examine the difference between the adiabatic and isothermal response. The tempera-

ture change affects $\chi(T)$, but since by symmetry this temperature-induced change must be at least quadratic in polarization, the distinction is manifested as an increase in the coefficient ξ for the adiabatic case. One can show simply,⁹ that

$$\xi_s - \xi_T = (T/3C_P)(d\chi/dT)^2,$$

where C_P is the specific heat per unit volume at constant polarization. We estimate the difference ($\xi_s - \xi_T$) to be at most a few percent for SrTiO₃ and KTaO₃; so we shall henceforth ignore the correction.

The linear response of the crystal is described by the coefficient χ which is independent of polarization but which may depend on temperature as well as external stress. In our Raman scattering experiments, the effective driving frequency ($\omega_i - \omega_s = \omega_{ph}$) is much higher than the electrostrictive response frequencies of the crystal. Therefore the appropriate χ for comparison of our results with the LST relation is the clamped χ . The fact that our data are in such good agreement with χ values obtained at much lower frequencies^{10,11} (the free χ) indicates that for SrTiO₃ and KTaO₃ the difference between the linear dielectric response at constant strain (clamped) and that at constant stress (free) is at most a few percent.

The temperature dependence of χ is quite striking in both SrTiO₃ and KTaO₃. At temperatures above 50°K, each material exhibits a paraelectric response with $\chi = \text{const} \times (T - T_c)$, i.e., the dielectric constant obeys a Curie-Weiss law $\kappa = C/(T - T_c)$. The infinity in κ is associated with a ferroelectric or antiferroelectric phase transition near T_c . In fact, neither KTaO₃ nor SrTiO₃ is known unambiguously to reach this phase transition. The Curie-Weiss behavior ceases to hold at lower temperatures, so that κ remains finite.

The constants ξ , ξ' , and ζ describe the nonlinear response of the crystal to electric fields. The signs of ξ and ξ' determine, of course, whether the response is initially more or less than linear, and, in addition, determine the order of the ferroelectric phase transition. Where ξ and ξ' are negative, the transition is first order (BaTiO₃, for example). Where ξ and ξ' are positive, as in KTaO₃ and SrTiO₃, the transition, if it were to occur, would be second order.

A cubic crystal is isotropic in its linear response, and this is reflected in the fact the linear-response term χ is a scalar. In the case that $\xi = \xi'$, the crystal is isotropic in its nonlinear response as well, at least to the terms in fourth order considered here.

The constants χ , ξ , and ξ' have previously been measured for SrTiO₃, and χ and ξ for KTaO₃, by more or less standard techniques for measuring di-

⁹ E. Fatuzzo and W. J. Merz, *Ferroelectricity* (John Wiley & Sons, Inc., New York, 1967).

¹⁰ H. E. Weaver, *J. Phys. Chem. Solids* **11**, 274 (1959).

¹¹ S. H. Wemple, *Phys. Rev.* **137**, A1575 (1965).

⁸ R. H. Lyddane, R. G. Sachs, and E. Teller, *Phys. Rev.* **59**, 673 (1941).

electric constants in the presence of biasing fields.¹⁰⁻¹⁵ The values obtained are compared with our measurements below.

The connection between the dielectric response of a crystal and its optical phonon frequencies was stated in an equation derived by Lyddane, Sachs, and Teller.⁸ For a diatomic crystal with a single IR-active lattice mode,

$$\kappa_{\infty}/\kappa = \omega_T^2/\omega_L^2,$$

where κ_{∞} and κ are the dielectric constants for frequencies, respectively, far above and far below the lattice-mode frequencies. This relation is valid, in general, when the damping of the modes is small.¹⁶ It has been generalized to the case of several optical modes:

$$\kappa_{\infty}/\kappa = \prod_i [(\omega_T)_i^2/(\omega_L)_i^2]. \quad (5)$$

For ferroelectric crystals, the dielectric constant is strongly temperature-dependent:

$$1/\kappa = (T - T_c)/C. \quad (6)$$

Fröhlich¹⁷ pointed out that the vanishing of $1/\kappa$ implied the vanishing of some transverse phonon frequency. Cochran² and Anderson¹⁸ have developed this idea further, and it is now known that in many crystals almost all the temperature dependence in the right-hand side of Eq. (5) is carried by a single transverse phonon frequency, the lowest-frequency mode, called variously the "soft mode," "ferroelectric mode," or "Cochran mode." The frequency of this mode in the harmonic approximation then goes to zero at $T = T_c$. The ferroelectric transition is thus simply understood as a displacement which resembles the ferroelectric mode, and therefore has become frozen in because the restoring force has vanished.

For our purposes, we simplify the LST relation as follows:

$$\omega_s^2 \kappa = \kappa_{\infty} \left[\prod_i (\omega_L)_i^2 / \prod_i' (\omega_T)_i^2 \right] = \text{const} \equiv A. \quad (7)$$

(\prod_i' is a product over all TO frequencies except the soft mode.) We shall be interested in comparing our measurements of ω_s^2 with electrical measurements of κ .

¹² D. Itschner, Promotionsarbeit, Eidgenössischen Technischen Hochschule in Zurich, 1965 (unpublished).

¹³ L. E. Cross and D. Chakravorty, in *Proceedings of the International Conference on Ferroelectricity* (Prague, 1966).

¹⁴ D. Kahng and S. H. Wemple, *J. Appl. Phys.* **36**, 2925 (1965).

¹⁵ G. Rupprecht, R. O. Bell, and B. D. Silverman, *Phys. Rev.* **123**, 97 (1961).

¹⁶ A. S. Barker, in *Ferroelectricity; Proceedings of a Symposium, Warren, Mich., 1966*, edited by E. F. Weller (Elsevier Publishing Co., Inc., New York, 1967).

¹⁷ H. Fröhlich, *Theory of Dielectrics* (Oxford University Press, London, 1949).

¹⁸ P. W. Anderson, in *Fizika Dielektrikov*, edited by G. I. Shansvi (Academy of Sciences of USSR, Moscow, 1960).

We have found Eq. (7) to be valid not only in the limit of small fields, but also in the presence of strong biasing fields. In either case, the relevant κ is the small signal incremental dielectric constant given in Eq. (3):

$$\omega_s^2 = A/\kappa \approx A/(\kappa - 1) \\ = A\epsilon_0 \{ \chi(T) + 3\xi P_z^2 + \xi'(P_x^2 + P_y^2) + 5\zeta P_z^4 \}. \quad (8)$$

(κ and $\kappa - 1$ are nearly equal, since $\kappa \geq 200$ for all temperatures.)

We have previously discussed the field-induced splitting of transverse optical modes. With field applied in the [001] direction, only $P_z = P$ is nonzero. The z-polarized or TO-parallel mode has a frequency related to the zz component of the inverse dielectric tensor:

$$(\omega_s^{\parallel})^2 = A\epsilon_0 [\chi(T) + 3\xi P^2 + 5\zeta P^4]. \quad (9)$$

The [110]-polarized or TO-perpendicular mode has a frequency related to the xx or yy component of the inverse dielectric tensor:

$$(\omega_s^{\perp})^2 = A\epsilon_0 [\chi(T) + \xi' P^2]. \quad (10)$$

III. EXPERIMENTAL TECHNIQUES AND APPARATUS

With the exception of the electric field application and synchronous detection of the scattered light, the apparatus used in these experiments—including temperature control—has been described previously.¹⁹ Linearly polarized light of 100–200 mW at 4880 or 5145 Å from an argon-ion laser is focused into the sample and light scattered through 90° is collected into the slit of a double Czerny-Turner spectrometer. By suitable positioning of rotators and polarizers, particular elements of the Raman scattering tensor are examined to determine the symmetry character of the vibration responsible for the scattering. A flowing-He-gas system is employed to cool the cold finger of a He Dewar upon which the sample is mounted. Temperatures between 8 and 300°K can be conveniently chosen and maintained to within a fraction of a degree. The sample chamber is evacuated to facilitate imposition of electric fields. The sample is provided with electrodes of evaporated layers of Au over Cr and held between In-faced Cu contacts. Sample temperature is monitored by thermocouples and GaAs diodes affixed to the sample block.

The photoelectric detection and amplification scheme employed is chosen according to the form of the imposed electric field. Two types of field imposition are employed: (a) a sinusoidal electric field at $\omega_{ac} = 210$ cps and (b) a repetitively pulsed electric field consisting of square voltage pulses 200 μsec long repeated every 3 to 100 msec. While method (a) is simpler and

¹⁹ P. A. Fleury and R. Loudon, *Phys. Rev.* **166**, 514 (1968).

more convenient, it does not yield simply interpretable quantitative results when the imposed fields are large enough that the response of the crystal is nonlinear. The region where the phonon frequency depends upon electric field is best explored by method (b).

The detection scheme for method (a) is based on the observation in Sec. II that the field-induced scattering intensity $I(E)$ is proportional to E^2 and hence should be modulated at $2\omega_{ac}$. Part of the signal from the sinusoidal signal generator (at ω_{ac}) is fed through a frequency doubler and used as a reference, at $2\omega_{ac}$, for a lock-in detector. Thus only that component of the scattered light whose intensity is modulated at $2\omega_{ac}$ appears on the recorder trace. The discrimination against the intense field-independent scattering due to two-phonon processes is virtually complete in this method. However, method (a) is inappropriate for quantitative measurements of the effect of electric field on phonon frequency or linewidth, since the instantaneous value of applied field varies between zero and $|E_{ac}|$. As we shall see in Sec. IV, electric fields can induce large changes in the phonon frequency. In addition, when the response of the crystal to E_{ac} is appreciably nonlinear, the scattered intensity ceases to vary as E_{ac}^2 so that the method is less valuable.

To obviate these difficulties, we employ method (b). Here part of the voltage-pulse output from a Velonex pulser is used to trigger a gated or "boxcar" integrator. The integrator accepts photocurrent from the photomultiplier only when the gate is open. Further, the duration of the integrator gate (50 μsec) is set to about one-fourth the duration of the applied voltage pulse, so that over the time viewed, the voltage on the crystal is constant and hence rather precisely defined. Discrimination against the intrinsic second-order scattering in method (b) is provided by (i) the

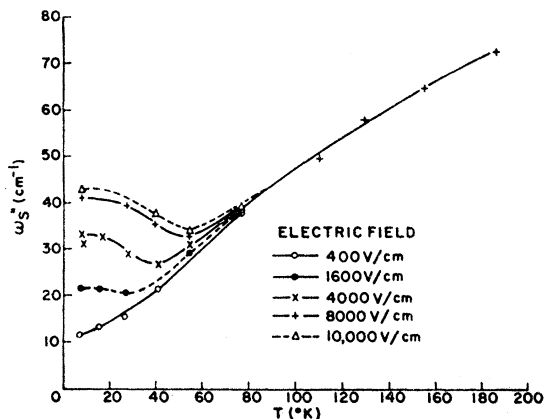


FIG. 3. Frequency of parallel component of the soft mode as a function of temperature in SrTiO_3 for various applied fields. The solid and dashed curves are drawn merely to connect data points.

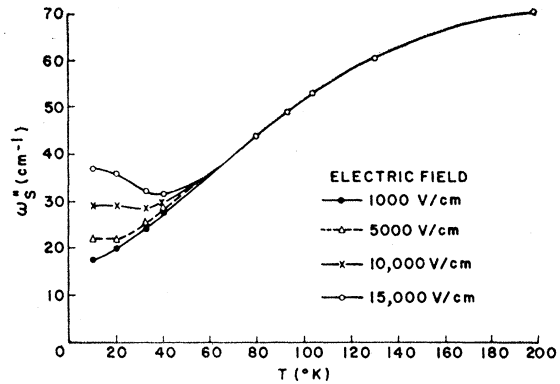


FIG. 4. Frequency of parallel component of the soft mode as a function of temperature in KTaO_3 for various applied fields. The solid and dashed curves are drawn merely to connect data points.

small duty cycle of the voltage pulses and (ii) an ac preamplifier placed between the phototube and the boxcar integrator. The low-frequency rolloff of the preamplifier is set to reject dc and low-frequency ($\lesssim 100$ cps) Fourier components of the photocurrent. Thus, because the Fourier components of the field-dependent scattered intensity range up to 5000 cps, whereas the intrinsic scattering has its components peaked at ~ 0 cps, a rather complete discrimination is effected. Another advantage of method (b) is the ability to control and minimize sample heating when the field strength is increased by varying the voltage-pulse repetition rate (duty cycle).

IV. EXPERIMENTAL RESULTS AND DISCUSSION

A. Temperature Dependence of Soft-Mode Frequencies

We reported earlier the observation of induced scattering from the "soft" or "ferroelectric" mode ω_s in KTaO_3 ²⁰ and SrTiO_3 ²¹ as well as the electric-field-induced frequency shift of ω_s in SrTiO_3 .²² Here we present more complete results for the field and temperature dependence of the frequency, linewidth, and induced scattering cross sections for the soft mode in these crystals. Figure 3 summarizes the frequency variation in SrTiO_3 for the soft-mode component parallel to the applied field. All data were taken by method (b). The temperature dependence of ω_s in absence of field is given approximately by the 400-V/cm line in Fig. 3. The frequency increases from 11 cm^{-1} at 8°K to 85 cm^{-1} at 250°K. Measurements were taken up to 250°K, although points above

²⁰ P. A. Fleury and J. M. Worlock, Phys. Rev. Letters **18**, 665 (1967).

²¹ J. M. Worlock and P. A. Fleury, Bull. Am. Phys. Soc. **12**, 662 (1967).

²² J. M. Worlock and P. A. Fleury, Phys. Rev. Letters **19**, 1176 (1967).

TABLE I. Phonon frequencies in cm^{-1} (Ref. 24).

	A'	η	$\omega_{\text{LO}}^{(1)}$	$\omega_{\text{TO}}^{(2)}$	$\omega_{\text{LO}}^{(2)}$	$\omega_{\text{TO}}^{(3)}$	$\omega_{\text{LO}}^{(3)}$	$\omega_{\text{TO}}^{(4)}$	$\omega_{\text{LO}}^{(4)}$
SrTiO_3	1.7×10^8	2.38	173	178	265	265	473	544	815
KTaO_3	1.28×10^8	2.15	118	199	290	290	423	549	833

200°K are not shown in Fig. 3, since it is intended to emphasize the electric field dependence. Figure 4 shows the analogous results for KTaO_3 , where the soft-phonon frequency increases from 18 cm^{-1} at 10°K to 85 cm^{-1} at 300°K (for low applied fields ~ 500 V/cm). We note that the low-temperature values of ω_s differ from those quoted in our original paper.²⁰ This difference is due partly to a difference in sample,²³ but is primarily due to the use of rather high (several kV/cm) sinusoidal fields in our original measurements. As seen from Fig. 4, ω_s increases as the applied field is increased. The agreement between the (low-field) temperature dependence of the soft mode that we observe and that expected from the LST relation and the dielectric-constant measurement of Wemple¹¹ (for KTaO_3) and Weaver¹⁰ (for SrTiO_3) is quite good in both materials.

In particular, not only is the temperature dependence

$$\omega_{\text{TO}}(T) = A' / [\kappa(T)]^{1/2}$$

well verified, but also the *absolute value* of A' is quite accurately given by

$$A' = \eta \omega_{\text{LO}}^{(1)} \frac{\omega_{\text{LO}}^{(2)} \omega_{\text{LO}}^{(3)} \omega_{\text{LO}}^{(4)}}{\omega_{\text{TO}}^{(2)} \omega_{\text{TO}}^{(3)} \omega_{\text{TO}}^{(4)}}$$

(where η is the refractive index) in both crystals, thus removing the necessity to normalize our data at one point—as was done in our earlier papers. The values that we used to calculate A' are summarized in Table I.²⁴ We emphasize that the soft-mode frequency does not reach zero; nor do we find any evidence for the ferroelectric phase transition in either SrTiO_3 or KTaO_3 . These are separate statements, since there is no requirement that a soft-mode frequency precisely vanishes in order for a phase transition to occur.

B. Electric-Field Dependence of Soft-Mode Frequencies

It is obvious that these two crystals are not only qualitatively identical but are also quantitatively quite similar. This similarity extends to their nonlinear properties, as exemplified by the electric field dependence of their soft-mode frequencies. Figures 5 and 6 show the observed field dependence at various temperatures for the soft mode in SrTiO_3 and KTaO_3 ,

respectively. In SrTiO_3 the induced scattering intensity from both components of the soft TO mode (phonon polarized \parallel and \perp to the applied field) was sufficient to allow observation over a wide range of fields. At 8°K the shift in the \parallel component ω_s^{\parallel} is most striking from a zero-field value of 10 to 44.5 cm^{-1} at 12 kV/cm. This variation follows that predicted by Eq. (9) in Sec. II, with $\chi = 3.7 \times 10^6$ and $\xi = 1.5 \times 10^{10}$ in mks units. The frequency variation for \perp component ω_s^{\perp} is less dramatic but still substantial—the 12-kV/cm value being 26 cm^{-1} . This implies $\xi' = 1.5 \times 10^{10}$ in Eq. (10). The symmetries of these components in the presence of a $[001]$ field were inferred from their nonzero Raman-tensor elements. For ω_s^{\parallel} we find that α_{zz} and $\alpha_{yy} = \alpha_{xx}$ are nonzero, implying A_1 symmetry. For ω_s^{\perp} we find $\alpha_{yz} = \alpha_{xy}$ nonzero, implying E symmetry.

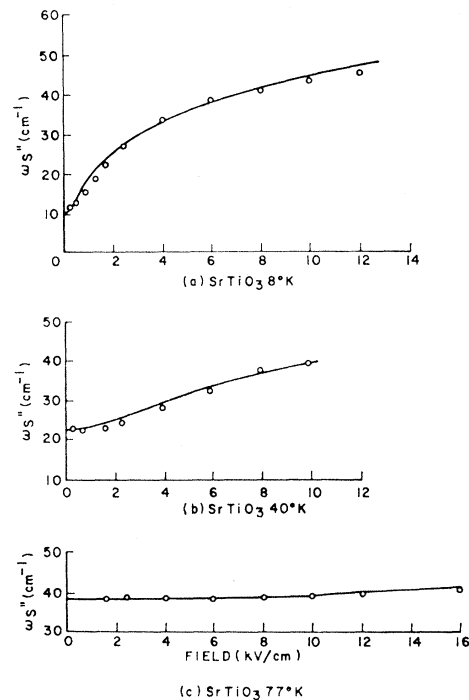


FIG. 5. Electric field dependence of the parallel component of the soft-mode frequency in SrTiO_3 at various temperatures. The solid lines are calculated from Eqs. (2) and (9), using the values of the parameters indicated (in mks units):

- (a) $T = 8^\circ\text{K}$, $\chi = 3.7 \times 10^6$, $\xi = 1.6 \times 10^{10}$;
- (b) $T = 40^\circ\text{K}$, $\chi = 15.5 \times 10^6$, $\xi = 0.9 \times 10^{10}$;
- (c) $T = 77^\circ\text{K}$, $\chi = 52.6 \times 10^6$, $\xi = 0.7 \times 10^{10}$.

²³ S. H. Wemple (private communication). At low temperatures the dielectric response of the crystal is quite sensitive to impurities.

²⁴ The phonon frequencies in this table are taken from Refs. 4–7.

The same symmetry rules obtain of course, in KTaO₃, although, as seen from Fig. 6, the phonon-frequency shift with applied field at a given temperature is smaller than in SrTiO₃. In KTaO₃ only the $\omega_s^{||}$ component could be followed, increasing from 18.1 cm⁻¹ at low fields to 37 cm⁻¹ at 13 kV/cm (for $T=10.6^\circ\text{K}$). Only at our highest fields could we observe the ω_s^+ component. At 15.2 kV/cm and $T=10^\circ\text{K}$, ω_s^+ is 23.5 cm⁻¹, while $\omega_s^{||}$ is 41.5 cm⁻¹. These observations imply $\chi=17.7\times 10^6$, $\xi=1\times 10^{10}$, $\xi'=1\times 10^{10}$, and $\zeta=4\times 10^{12}$. These nonlinear coefficients were evaluated by fitting the observed electric-field dependence of $\omega_s^{||}$ and ω_s^+ to numerical solutions of Eqs. (2), (9), and (10). Figures 5 and 6 illustrate these evaluations for various temperatures in both SrTiO₃ and KTaO₃. The values of $\chi(T)$ used at the various temperatures are within a few percent of the values previously obtained by conventional dielectric methods.^{10,11} Note that some temperature dependence is indicated for the ξ and ζ coefficients. Generally, ξ decreases as the temperature is increased in both SrTiO₃ and KTaO₃. However, the values of these nonlinear coefficients are uncertain by as much as 30% for ξ and a factor of 2 for ζ . While greater accuracy in these values might result from a systematized curve-fitting procedure—such as a least-squares analysis—no such procedure was employed here. The

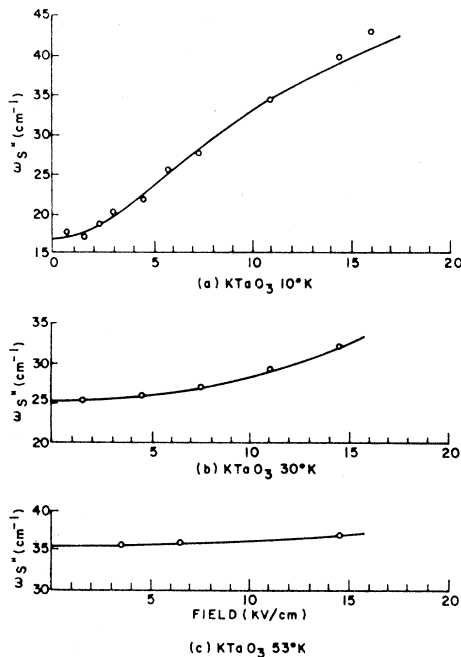


FIG. 6. Electric field dependence of the parallel component of the soft-mode frequency in KTaO₃ at various temperatures. The solid lines are calculated from Eqs. (2) and (9), using the values of the parameters (in mks units) indicated:

- (a) $T=10^\circ\text{K}$, $\chi=17.7\times 10^6$, $\xi=1.0\times 10^{10}$, $\zeta=4\times 10^{12}$;
- (b) $T=30^\circ\text{K}$, $\chi=41.3\times 10^6$, $\xi=0.5\times 10^{10}$, $\zeta=3\times 10^{12}$;
- (c) $T=53^\circ\text{K}$, $\chi=80.5\times 10^6$, $\xi=0.5\times 10^{10}$, $\zeta=4\times 10^{12}$.

curves in Figs. 5 and 6 were obtained by varying χ , ξ , and ζ until satisfactory visual fits to the data were found.

Previous measurements of the nonlinear dielectric response of SrTiO₃ in the frequency range of 1–36 kHz have been made at various temperatures. Itschner¹² found $\xi=6.3\times 10^9$ and $\xi'=4.5\times 10^9$ for $0<T<90^\circ\text{K}$. Rupprecht, Bell, and Silverman¹⁵ obtained $\xi=7.6\times 10^9$ and $\xi'=2.8\times 10^9$ for $90\leq T\leq 230^\circ\text{K}$. Cross and Chakravorty¹³ obtained $\xi=9.5\times 10^9$ for $18\leq T\leq 60^\circ\text{K}$. These compare very favorably with our values of ξ in Fig. 5. Where we have been able to measure ξ' (at 8°K), we found $\xi=\xi'$.

The data on KTaO₃ are less extensive. Kahng and Wemple¹⁴ have analyzed their data taken at 100 kHz, using only the first nonlinear term in dielectric response, and obtain $\xi=9\times 10^9$ at 4.2°K and $\xi=4\times 10^9$ at 295°K . These values compare very well with ours shown in Fig. 6. However, our data require a non-zero value for ζ equal to $\sim 4\times 10^{12}$.

C. Temperature and Electric Field Dependence of Soft-Mode Scattering Cross Sections

The electric field dependence of the induced scattering cross section for the soft mode was observed to be quadratic at 77°K in both KTaO₃ and SrTiO₃. At 10°K , quadratic dependence was also found at low fields in KTaO₃.

Similar checks at low fields in SrTiO₃ yielded a quadratic dependence. However, at higher fields—when nonlinear terms in the response of the crystal becomes important—the induced scattering intensity increases less rapidly than E^2 . In SrTiO₃ at low temperatures the field dependence of the soft-mode cross section is complicated by a strong mode coupling that we shall discuss below.

As reported earlier for KTaO₃,²⁰ the electric-field induced cross section (integrated over the phonon linewidth) for a given value of applied field increases by a factor of 10 when T is lowered from 300 to 80°K and by another factor of 10 between 80 and 8°K . We compared the induced cross section to the cross section of the 992-cm^{-1} line in liquid C₆H₆ and found that at 300°K and 14 kV/cm the KTaO₃ line is about 20 times weaker, corresponding to an extinction coefficient of $\sim 5\times 10^{-8}$ per cm of path length. Similar behavior obtains for SrTiO₃ when the fields at low temperatures are small enough that the response of the crystal to electric fields is essentially linear.²⁵

D. Soft-Mode Linewidths

One of the most interesting results to emerge from these experiments is a measurement of the linewidth

²⁵ V. Dvorak [Phys. Rev. 159, 652 (1967)] has calculated the electric-field-induced Raman effect for crystals of the SrTiO₃ type and has related the scattering cross sections to electro-optic coefficients of such materials.

TABLE II. Soft-mode frequencies and linewidths compared for IR and field-induced Raman experiments.

	Raman (present work)			Infrared	
	ω_s (cm^{-1})	Γ_s (cm^{-1})	T ($^\circ\text{K}$)	ω_s (cm^{-1})	Γ_s (cm^{-1})
SrTiO ₃	90	17	300	88 ^a	35.2 ^a
	41	3	85	44 ^a	61.7 ^a
	10	<0.5	8
KTaO ₃	88	20	300	85.1 ^b	46.5±9 ^b
	43	7.5	80	58±5 ^c	...
	18	1.3	10	25 ^d	...

^a Reference 4.^b Reference 5.^c Unpublished results of Boyd and Miller quoted by Barker (Ref. 16).^d Reference 33.

of the ferroelectric mode. Both KTaO₃ and SrTiO₃ have been studied using far-IR reflection, from which studies one characteristically infers a frequency, a linewidth, and a strength for each phonon mode.^{4,5} A main point of this section is to indicate the extreme discrepancy between linewidths obtained in the IR experiments and those that we measure in the induced Raman scattering.

Although IR measurements in KTaO₃ and SrTiO₃ have been made at only a few temperatures, the data are sufficient to show convincingly the large discrepancy with our Raman measurements. Comparison is made in Table II. The linewidth Γ_s is full width at half-maximum. Note that in every case there is a discrepancy of at least a factor of 2. The errors in our linewidth determination are of the order of 1 cm^{-1} and arise chiefly from the subtraction procedure, so they do not affect our discussion in this section.

Our procedure for extracting the phonon linewidth Γ_p from the total width Γ_t was an intermediate between the direct subtraction of the instrumental (Lorentzian combination) and the difference between the squares of the total and instrumental widths Γ_I (Gaussian combination). The formula used was $\Gamma_t^2 = \Gamma_p^2 + \Gamma_I^2 - 2\Gamma_p\Gamma_I \cos\varphi$. When $\varphi = \pi$ and $\frac{1}{2}\pi$, the above reduces to the Lorentzian and Gaussian methods, respectively. By varying Γ_I , we determined that $\cos\varphi = -0.72$ was a "good" value for our experiments.

The discrepancies between the Raman and the IR linewidths are extremely large in some cases. Consider, for example, SrTiO₃ at 85°K in Table II. While the two methods yield essentially the same values of soft-mode frequency (41 and 44 cm^{-1}), the Raman linewidth is only 3 cm^{-1} , some 20 times smaller than the IR value of 61.7 cm^{-1} . Indeed, depending upon which value one accepts, one is forced to opposite conclusions as to whether or not the mode is overdamped. As is evident from Tables II and III, the linewidths measured by the IR technique are larger

without exception than those measured for the same phonons by the Raman method.

The analysis of the IR-reflectivity experiments typically involves use of a model—usually a classical oscillator characterized by a resonant frequency, a damping constant, and an oscillator strength—upon which a calculation of frequency-dependent reflectivity is based. If there are additional physical processes contributing to the IR response, such as multiple-phonon processes or additional IR-active modes, which are not included in the model, one would infer erroneous values for the parameters of the model oscillators. As we have shown elsewhere,²⁶ there is some evidence that at low temperatures in SrTiO₃ there are additional IR-active zone-center phonons not accounted for in previous analyses.²⁷ Multiple-phonon processes, of course, could also contribute in both SrTiO₃ and KTaO₃.

Because the procedure for extracting frequency and linewidth information from the experimental data is so much simpler and more direct in the Raman than in the IR experiments, we believe that the former results are more reliable. We shall therefore compare our linewidths with some calculated lifetimes for soft-phonon modes.

The temperature dependence of soft-mode linewidths in the displacive ferroelectrics has received some theoretical attention. The recent calculation of Tani²⁸ presupposes a ferroelectric phase transition in SrTiO₃ at $T_0 = 32^\circ\text{K}$ and accordingly predicts Γ_s proportional to $T/(T-T_0)^{1/2}$. It is clear from our data on both SrTiO₃ and KTaO₃ (Fig. 7) that neither of these materials exhibits such a temperature dependence for the linewidth. Dvorak²⁹ has also treated the problem in terms of third-order phonon interactions. He argues that in SrTiO₃ at temperatures between 10 and 50°K the dominant contribution to the soft-mode linewidth arises from a three-phonon process in which a soft optic phonon scatters from an acoustic phonon to produce another optic phonon. In evaluat-

TABLE III. Comparison of IR and Raman measurements for TO modes other than the soft mode at lower temperatures in SrTiO₃.

	ω (cm^{-1})	Γ (cm^{-1})	T ($^\circ\text{K}$)	Method
SrTiO ₃	172.5	6.9	85	IR (Ref. 4)
	171	<2	47	Raman (present work)
	544	24	85	IR (Ref. 4)
	560	5	47	Raman (present work)

²⁶ P. A. Fleury, J. F. Scott, and J. M. Worlock, Phys. Rev. Letters **21**, 16 (1968).²⁷ A. S. Barker and J. J. Hopfield, Phys. Rev. **135**, A1732 (1964).²⁸ K. Tani, Phys. Letters **25A**, 400 (1967).²⁹ V. Dvorak, Czech. J. Phys. **B17**, 726 (1967).

ing the temperature dependence of his linewidth, Dvorak does not assume a Curie-type temperature dependence for the soft-mode frequency—as does Tani. Instead, he evaluates $\Gamma_s(T)$ in terms of $\omega_s(T)$ as inferred from dielectric-constant measurements. The agreement between his predictions and our observations is quite good—at least for T less than 50°K (see Table IV).

For $T > 50^\circ\text{K}$, Dvorak's calculations predict a decrease in Γ_s with increasing T , contrary to observations. In addition, it is likely that the agreement between our experiment and Dvorak's theory in the 10 – 50°K range is somewhat fortuitous, because his theory fails to incorporate two additional recently identified soft low-frequency phonons in SrTiO_3 .²⁶ Dvorak's calculation should therefore be more appropriate to KTaO_3 ; however, the experiment and theory are in poorer agreement for this material than

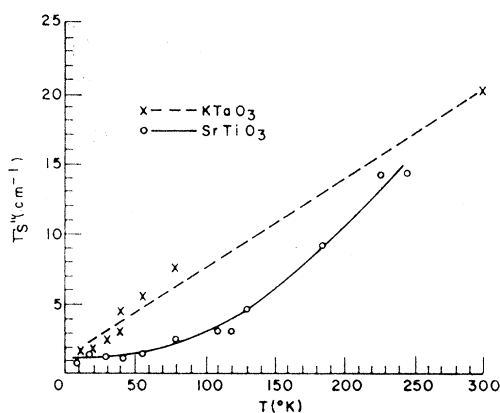


FIG. 7. Full width at half-maximum of the parallel component of the soft modes at various temperatures. Solid line is drawn through SrTiO_3 data points, dashed line through KTaO_3 data points.

for SrTiO_3 . In KTaO_3 , Γ_s seems well approximated by a linear T dependence, while in SrTiO_3 , the temperature dependence is roughly given by $T^{3/2}$ (see Fig. 7). Note that no large discontinuities in Γ_s for SrTiO_3 were observed at any temperature between 10 and 240°K —not even at 110°K , where the well-known phase transition from tetragonal to cubic symmetry occurs.³⁰ It seems proper to say that the linewidth of soft modes in such perovskites deserves more theoretical investigation.

E. Modes other than Soft Mode

As pointed out in Sec. II, the application of an electric field along the $[001]$ direction imparts a C_{4v} symmetry to the perovskite crystal and should make every phonon first-order Raman-active. This section reports our observation of field-induced scattering from some of the modes other than the soft modes

³⁰ F. W. Lytle, J. Appl. Phys. **35**, 2212 (1964).

TABLE IV. Observed and calculated soft-mode linewidths in cm^{-1} at various temperatures in SrTiO_3 .

T ($^\circ\text{K}$)	10	20	30	40	50
Γ_s (calc)	1	2	2.5	2.4	2.25
Γ_s (obs)	0.8	1.3	1.1	1.0	1.5

and compares our results with those of IR and neutron techniques. We shall also comment briefly on the intrinsic Raman spectrum of SrTiO_3 and the possibility of a phase transition.

KTaO_3 . Previous reports of the intrinsic Raman spectrum of KTaO_3 ^{31,32} have correctly interpreted this spectrum at all temperatures between 4 and 473°K as second order. The only direct knowledge of zone-center phonon frequencies for KTaO_3 prior to this work are from the IR-reflectivity studies by Miller and Spitzer⁵ and by Perry and McNelly³³ and from a neutron scattering study of the soft-mode frequency by Shirane *et al.*⁷ The IR experiments give at room-temperature frequencies as listed in column I of Table V.

In column II are the frequencies that we observed in the electric-field-induced scattering experiments. Even though all the phonons are Raman-active by symmetry, the field-induced cross section is sufficiently strong to permit observation for only the soft mode, the 198 -, and the 556 - cm^{-1} TO. Column III shows the 300°K soft-mode frequency obtained by neutron scattering.⁷ Note that the "silent mode" (ω_{L2} , ω_{T3}) has not been observed by any technique in KTaO_3 .

SrTiO_3 . The data of all sorts are more complete in SrTiO_3 . Barker¹⁶ has done the IR at two tem-

TABLE V. Phonon frequencies in cm^{-1} at 300°K in KTaO_3 as measured by various techniques.

	I (IR) ^a	II (Raman) ^b	III (Neutron) ^c
ω_{T1}	85.1	85	86
ω_{L1}	196
ω_{T2}	199	198 (10°K)	...
ω_{L2}
ω_{T3}
ω_{L3}	435
ω_{T4}	549	556 (10°K)	...
ω_{L4}	910

^a Reference 5.

^b Present work.

^c Reference 7.

³¹ C. H. Perry, J. H. Fertel, and T. F. McNelly, J. Chem. Phys. **47**, 1619 (1967).

³² W. G. Nilsen and J. G. Skinner, J. Chem. Phys. **47**, 1413 (1967).

³³ C. H. Perry and T. F. McNelly, Phys. Rev. **154**, 456 (1967).

TABLE VI. Phonon frequencies in SrTiO₃ in cm⁻¹ as measured by various techniques.

	I (IR) (85°K) ^a	II (Raman) ^b	III Neutron (90°K) ^c
ω_{T1}	44	40 (80°K)	42
ω_{L1}	171	...	168
ω_{T2}	172	173 (47°K)	168
ω_{L2}	...	268 (10°K)	262
ω_{T3}	...	268 (10°K)	262
ω_{L3}	470
ω_{T4}	544	560 (47°K)	...
ω_{L4}	801

^a Reference 4.^b Present work.^c Reference 6.

peratures (300 and 85°K), while Cowley⁶ has done extensive neutron experiments at 90 and 296°K. In addition, the electric-field-induced Raman effect has yielded more phonon frequencies than for KTaO₃. The table summarizes the results.

We have observed field-induced Raman scattering from all the TO modes in SrTiO₃, although apparently from none of the LO modes. Our experiments could not distinguish between degenerate TO and LO modes, so that it is possible that the lines at 173 and 268 cm⁻¹ are in part due to ω_{L1} and ω_{L2} . Except for the lowest temperatures at frequencies in the vicinity of the soft mode, the only features in the field-induced spectrum are those appearing in the table. Their frequencies and polarization selection rules leave no doubt that these are the zone-center phonons observed in neutron scattering and IR experiments. Note that we have even observed the so-called *silent* mode in SrTiO₃ (at 268 cm⁻¹).

While there is no question that the lines that we observed in the field-induced scattering are first order, there has been some question as to whether there may be other zone-center phonons not appearing anywhere in Table VI. Consider Fig. 8, which displays the intrinsic Raman spectrum of SrTiO₃ at (a) 300 and (b) 30°K. Note the three sharp features at 48, 146, and 459 cm⁻¹ apparent in (b) but absent in (a). Recent observers of the low-temperature intrinsic Raman spectrum of SrTiO₃ have identified these lines as first order Raman lines made allowed and shifted in frequency by some unidentified departure from the perovskite structure.^{34,35} However, we have already accounted for all the known zone-

center phonons in the perovskite structure by the field-induced scattering experiments and have shown that these do not correspond to the above mentioned lines. In addition, examination of the intrinsic spectrum of SrTiO₃ at low temperatures reveals a fourth sharp feature at 15 cm⁻¹. Thus in all there are four new "modes" at low temperatures in SrTiO₃—in addition to the phonons present in the high-temperature region.

We have recently considered the evidence from electron-spin-resonance and sound-velocity measurements together with the intrinsic Raman spectra in SrTiO₃ and have proposed a microscopic model of the 110°K phase transition that accounts for all these observations.²⁶ As T_c is approached from above in the cubic phase, the frequency of the zone-corner (R -point) F_{2u} phonon softens. At $T_c=110^\circ\text{K}$ the R point becomes a reciprocal-lattice point of the new Brillouin zone—resulting in a unit cell twice as large as that above T_c . Several new zone-center phonons appear as a result of the unit-cell doubling. Of these the Raman-active modes are the sharp lines in the intrinsic spectrum mentioned above. This model of the phase transition explains not only the existence of the sharp lines, but also their symmetries, temperature dependence, and interactions with components of the soft ferroelectric mode in the presence of an applied field. Additional predictions and details of the model are presented in Ref. 26.

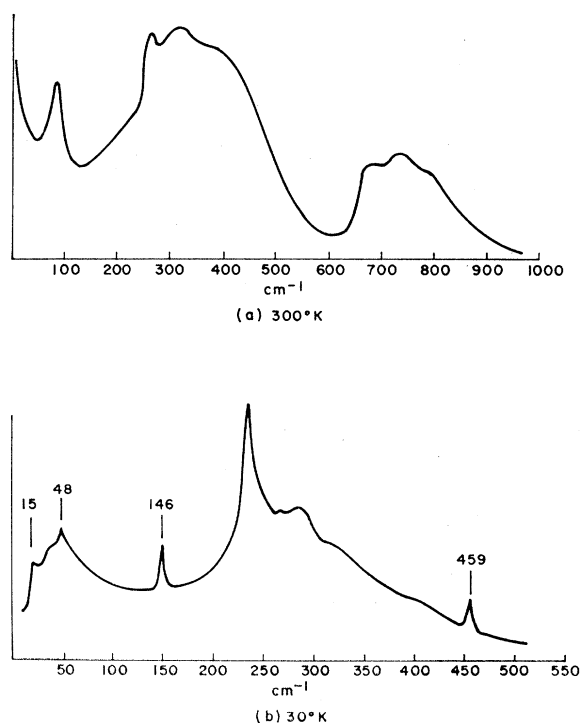


FIG. 8. Intrinsic Raman spectrum (i.e., taken with no field applied) of SrTiO₃ at (a) room temperature and (b) 30°K.

³⁴ D. C. O'Shea, R. V. Kolluri, and H. Z. Cummins, *Solid State Commun.* **5**, 387 (1967); R. F. Schaufle and M. J. Weber, *J. Chem. Phys.* **46**, 2859 (1967); L. Rimai and J. L. Parsons, *Solid State Commun.* **5**, 381 (1967).

³⁵ W. G. Nilsen and J. G. Skinner, *J. Chem. Phys.* **48**, 2240 (1968).

F. Field-Induced Scattering Cross Sections

We have already discussed the field and temperature dependence of the soft modes in SrTiO₃ and KTaO₃. Here we present the values of induced cross sections for other phonons relative to these. Again we discuss KTaO₃ first. Besides the parallel component of the soft mode, we were able to observe three other induced scatterings in KTaO₃, and these at low temperatures (10°K) and high fields (15 kV/cm). Here we found the perpendicular soft-mode component ω_s^\perp to have a cross section relative to the parallel component of $\sigma_s^{zz}=0.04\sigma_s^{zz}$; the TO phonon at 198 cm⁻¹ has $\sigma_{198}^{zz}=0.06\sigma_s^{zz}$; the TO phonon at 556 cm⁻¹ (polarized α_{zz}) is $\sigma_{566}^{zz}=0.05\sigma_s^{zz}$.

For SrTiO₃, σ_s^{zz} is about twice as large as σ_s^{zz} for KTaO₃ (at 5000 V/cm and 10°K) and, except in regions of interaction with the mode discussed above, exhibits similar E and T dependence. The perpendicular component of the soft mode (at 8°K and 5000 V/cm) has a relative cross section $\sigma_s^{zz}=0.13\sigma_s^{zz}$. The TO mode at 173 cm⁻¹ has been observed in two components also: $\sigma_{173}^{zz}=0.017\sigma_s^{zz}=14\sigma_{173}^{zz}$. The silent mode has $\sigma_{268}^{zz}=0.006\sigma_s^{zz}$. Finally, the 560 cm⁻¹ TO phonon has $\sigma_{560}^{zz}=0.013\sigma_s^{zz}$.

Dvorak²⁵ does not calculate explicitly any induced cross sections for modes other than the soft mode, but estimates that the relative cross sections for soft and nonsoft modes should go as $\sigma_{ns}/\sigma_s \sim \omega_s^2/\omega_{ns}^2$. Our experiments do not bear out this relation.

V. SUMMARY

We have presented methods and observations relevant to a new technique for studying odd-parity phonons in solids. There seem to be two realms of interest connected with this work: (a) the technique itself and (b) specific information obtained regarding ferroelectric perovskites. In general, the technique of electric-field-induced Raman scattering should permit study of IR-active and "silent" modes in crystals of high symmetry. In particular, the linewidths (or phonon lifetimes) are more simply and more reliably obtained by this method than by the IR-reflectivity experiments. The field-induced scattering cross sec-

tions that we observed in SrTiO₃ and KTaO₃ imply that, with attainable laboratory fields, even crystals with rather low ϵ 's can be studied. The field-induced scattering technique is also useful in discriminating against multiple-phonon scattering processes that contribute to the intrinsic spectrum.

With regard to the ferroelectric perovskites themselves, we have seen that the electric-field-induced scattering yields results which agree quite well with those obtained from IR and neutron experiments (except for the IR-linewidth values), as well as with dielectric measurements of the linear and nonlinear dielectric properties. The observed electric field dependence of the soft-mode frequency provides a microscopic basis for the macroscopic nonlinear dielectric behavior and thus verifies the generalized LST relation. In addition, it has permitted us to observe direct interaction between phonon modes in SrTiO₃. The field-induced Raman experiments in SrTiO₃ provide evidence for the model of the 110°K phase transition discussed in Ref. 26. Finally, the directly observable and electric-field tunable optic phonon mode should be useful in several ways. Electric field tunable Raman lasers and IR modulators are now possible. Certain transport properties of the medium—such as thermal conductivity³⁶ and electrical conductivity—can be markedly effected by changing the soft-phonon frequency. One also expects the soft mode to influence the acoustic properties of the medium via optic-acoustic phonon interactions.

ACKNOWLEDGMENTS

We are grateful to A. S. Barker, J. F. Scott, G. Shirane, and S. H. Wemple for illuminating discussions during the course of this work. We also thank A. S. Barker and S. H. Wemple for samples of SrTiO₃ and KTaO₃, H. L. Carter and D. H. Olson for expert technical assistance, and W. Pleibel and T. W. Armstrong for crystal preparation. It is a pleasure to acknowledge helpful comments on the manuscript from M. DiDomenico and I. P. Kaminow.

³⁶E. F. Steigmeier, Phys. Rev. **168**, 523 (1968). We thank Dr. Steigmeier for communicating his results to us prior to publication.